Title

Defining human ERAD networks through an integrative mapping strategy.

Journal

Nature cell biology, 14(1)

ISSN

1465-7392

Authors

Christianson, John C
Olzmann, James A
Shaler, Thomas A
et al.

Publication Date

2011-11-01

DOI

10.1038/ncb2383

Peer reviewed

HHS Public Access

Author manuscript

Nat Cell Biol. Author manuscript; available in PMC 2012 July 01.

Published in final edited form as:

Nat Cell Biol. ; 14(1): 93–105. doi:10.1038/ncb2383.

Defining human ERAD networks through an integrative mapping strategy

John C. Christianson[1,2,6], **James A. Olzmann**[1,6], **Thomas A. Shaler**[3], **Mathew E. Sowa**[4], **Eric J. Bennett**[4,5], **Caleb M. Richter**[1], **Ryan E. Tyler**[1], **Ethan J. Greenblatt**[1], **J. Wade Harper**[4], and **Ron R. Kopito**[1]

[1]Department of Biology & Bio-X Program, Stanford University, Lorry Lokey Bldg., 337 Campus Drive, Stanford, California 94305, USA

[2]Ludwig Institute for Cancer Research, University of Oxford, ORCRB, Headington, Oxford, OX3 7DQ, UK

[3]SRI International, Menlo Park, California 94025, USA

[4]Department of Cell Biology, Harvard Medical School, Boston, Massachusetts 02115, USA

SUMMARY

Proteins that fail to correctly fold or assemble into oligomeric complexes in the endoplasmic reticulum (ER) are degraded by a ubiquitin and proteasome dependent process known as ER-associated degradation (ERAD). Although many individual components of the ERAD system have been identified, how these proteins are organised into a functional network that coordinates recognition, ubiquitination, and dislocation of substrates across the ER membrane is not well understood. We have investigated the functional organisation of the mammalian ERAD system using a systems-level strategy that integrates proteomics, functional genomics, and the transcriptional response to ER stress. This analysis supports an adaptive organisation for the mammalian ERAD machinery and reveals a number of metazoan-specific genes not previously linked to ERAD.

Keywords

ER-associated degradation (ERAD); Hrd1; FAM8A1; UBAC2; mammalian EMC; CompPASS analysis; interaction network

Correspondence should be address to R.R.K. Phone: 650-723-7581, FAX: 650-724-4927, kopito@stanford.edu.

[5]current address: Division of Biological Sciences, UC San Diego, La Jolla, California 92093

[6]These authors contributed equally to this work

AUTHOR CONTRIBUTIONS

The manuscript was written collectively by J.C.C., J.A.O., and R.R.K. Experiments and data analysis were performed by J.A.O. and J.C.C. with assistance from C.M.B, R.E.T., and E.J.G. LC-MS/MS analysis was carried out by T.A.S. *CompPASS* analysis was performed by M.E.S. and E.J.B with support from J.W.H.

INTRODUCTION

Approximately one-third of the eukaryotic proteome consists of secreted and integral membrane proteins that are synthesised and inserted into the endoplasmic reticulum (ER), where they must correctly fold and assemble in order to reach functional maturity[1]. ER quality control (ERQC) refers to the processes simultaneously monitoring deployment of correctly folded proteins and assembled complexes to distal compartments, while diverting folding-incompetent, mutant or unassembled polypeptides for proteasomal degradation via the process of ER-associated degradation (ERAD, reviewed in[2–4]). An ever growing list of sporadic and genetic human disorders have been associated with ERQC, illustrating the pivotal role these processes play in governance of protein trafficking[5].

Many of the individual components thought to underlie ERAD have been identified through genetic and biochemical analyses in *S. cerevisiae* and mammals[4,6] and point toward a mechanism mediated by a network of topologically and compartmentally restricted, partially redundant protein complexes[2,4,7–9]. ERAD is a vectorial process whereby coordination of ERAD components across three subcellular compartments (ER lumen, lipid bilayer, and cytoplasm) must occur in order to effectively distinguish, target, and deliver misfolded substrates for degradation. Exclusion of the ubiquitin (Ub)-proteasome system (UPS) from the ER lumen necessitates that substrates traverse the ER membrane in order to be degraded, yet the molecular identity and mechanism of the required dislocation apparatus remains controversial[7,10,11].

Ub E3 ligases play central functional and organisational roles in ERAD[9]. In yeast, the E3s Hrd1p and Doa10p, which contain cytoplasmically oriented RING domains that recruit distinct Ub-conjugating enzymes and form functional complexes by scaffolding shared ERAD-related factors[12–16], appear to be sufficient to degrade all ERAD substrates[16,17]. ERAD substrates with luminal (ERAD-L) or membrane (ERAD-M) folding lesions utilise Hrd1p[16,18], while those with cytoplasmic lesions (ERAD-C) rely on Doa10p[16,17,19]. In contrast to yeast, at least 10 different E3s have been implicated in mammalian ERAD[20], possibly reflecting an evolutionary adaptation to the broader substrate range imposed by the more complex metazoan proteome. Three mammalian E3s, gp78, Hrd1, and TEB4, share similar domain and topological organisation, but scant sequence homology, with their yeast orthologs Hrd1p (ortholog of gp78 and Hrd1) and Doa10p (ortholog of TEB4). Uncovering how the organisation of E3-containing membrane complexes allows them to access substrates in the ER lumen/membrane and recruit the cytoplasmic dislocation/extraction apparatus is crucial to establishing a comprehensive understanding of ERAD.

In this work we have employed a systematic, multi-layered approach that integrates high-content proteomics, functional genomics, and gene expression to elucidate the interconnectivity and organisation of ERAD in mammals (Supplementary Fig. S1). These studies have allowed us to generate the first integrated physical and functional map of the ERAD system in the mammalian ER.

RESULTS

Mapping the mammalian ERAD interaction network

We employed a high-content proteomics strategy to map the mammalian ERAD interaction network, starting with 15 S-tagged baits consisting of proteins previously identified as ERAD pathway components in biochemical studies or by orthology to components identified in yeast (Supplementary Table S1, PRIMARY). After confirming ER localisation in HeLa cells (Supplementary Fig. S2) and stable expression of each full-length S-tagged bait in HEK293s (data not shown), protein complexes captured by S-protein affinity purification from detergent-solubilised lysates were analysed by liquid chromatography/ tandem mass spectrometry (LC-MS/MS). Interactions were initially assessed for all baits by independently analysing pull-downs from cells lysed in digitonin (DIG; Supplementary Table S2) or the more stringent detergent Triton X-100 (TX-100; Supplementary Table S3). Total spectral counts for each captured protein were subsequently evaluated with the Comparative Proteomics Analysis Software Suite (*CompPASS;* Supplementary Methods)[21,22]. *CompPASS* employs a database of interacting proteins (including data from baits in this study and 102 unrelated proteins described previously[21]) and comparative metrics to determine the likelihood of validity of interactors. The *CompPASS* parameter WD^N-score[22], which integrates the abundance, uniqueness, and reproducibility of an interacting protein, was used to identify High-confidence Candidate Interacting Proteins (HCIPs) for the ERAD network. Previous studies demonstrated that >68% of identified HCIPs were validated in subsequent biochemical analyses[21], a rate of validation that is well above other high throughput approaches to study protein-protein interactions[23]. In our study, interacting proteins surpassing a stringent threshold score of $WD^N > 1.0$ were designated as HCIPs (Supplementary Tables S2a and S3a). Interacting proteins scoring below this cut-off may still represent bona fide interactions (full list in Supplementary Tables S2b and S3b).

In addition to revealing interconnections among primary baits, this analysis uncovered 10 HCIPs with no prior relationship to ERAD. Seven (FAM8A1, UBAC2, KIAA0090, TTC35, C15orf24, TMEM111, and COX4NB) are functionally uncharacterised open reading frames (ORFs) and two (E-Syt1 and MMGT1) are implicated in cellular processes unrelated to quality control. The HCIP TXD16 (also known as ERp90) was recently suggested to be involved in ERAD[24]. Based on their identification as HCIPs with multiple ERAD components in both DIG and TX-100, high spectral counts, and predicted ER localisation (criteria described in Methods), these 10 HCIPs were introduced into the proteomic workflow to iteratively expand and validate the network (Supplementary Fig. S1, SECONDARY). Three proteins previously implicated in mammalian ERAD (TEB4, RNF5, and HERP) could not be sufficiently expressed and were omitted. Ultimately, our ERAD network analysis included 25 baits, of which 9 appear to be unique to metazoans. No correlation was observed between bait abundance and the total number of interactions and HCIPs identified (Supplementary Fig. S3a). From 3,325 individual proteins identified by MASCOT in DIG and 2,971 in TX-100 (Supplementary Tables S2b and S3b), *CompPASS* identified 320 and 202 HCIPs, respectively for the 25 baits (Supplementary Tables S2a and S3a). These HCIPs correspond to 143 and 97 non-redundant proteins with 71 HCIPs of interest, previously uncharacterised for a role in ERAD (see Online Methods for selection

criteria, Supplementary Table S4 and Fig. S3b). Over 50% of HCIPs are ER/membrane localised, and gene ontology (GO) analysis indicates diverse functionality with significant overrepresentation in folding, Ub and catabolic processes (Supplementary Fig. S3c and d).

Overview of the mammalian ERAD interaction network

Unbiased hierarchical clustering of all HCIPs identified for each bait in both detergents was used to assemble interaction data into a coherent network (Fig. 1). Four of the DIG clusters define subnetworks organised around the E3s Hrd1 (clusters 1D and 6D) and gp78 (clusters 3D and 8D), indicating a central role in organisation of the mammalian ERAD system. Both Hrd1 and gp78 clustered with established integral membrane, luminal, and cytoplasmic ERAD components (clusters 1D and 8D) as well as, separately, with most 26S proteasome subunits (clusters 3D and 6D). Cluster 2D defines a macromolecular complex of previously uncharacterised proteins that we have designated the mammalian ER Membrane Complex (mEMC, discussed below) to reflect its orthology to a complex associated with the unfolded protein response (UPR) in yeast[25]. Cluster 4D confirms the previously reported interactions of the AAA+ ATPase VCP/p97 with an integral membrane binding partner VIMP[26,27] and cytosolic NGly1[28], while revealing novel interactions of VIMP and UBXD2 with the VCP/p97 accessory protein UBE4A, a Ufd2 ortholog implicated in Ub chain extension[29]. In addition to confirming the ERFAD-SEL1L interaction[30], cluster 5D validated the recently reported interaction of ERFAD with TXD16/ERp90[24], reinforcing the connection between ERAD and oxidative protein folding/unfolding. Cluster 7D contains several novel HCIPs in complex with Derlin-1 and Derlin-2, including the Ca^{2+}-sensing protein extended-synaptotagmin 1 (E-Syt1)[31], the Ras superfamily member ARL6IP and YIF1B, both implicated in protein trafficking[32,33].

Of the 8 prominent clusters identified in DIG-solubilised cells, only cluster 2 remained intact with TX-100 lysis. Four clusters (1, 3, 5, 8) were fragmented into discrete sub-clusters, and three (4, 6, 7) were fully disrupted. Based on these clusters (Fig. 1), we merged individual interactomes (Supplementary Fig. S4) to construct a topologically rendered, detailed interaction map of the mammalian ERAD network in DIG and TX-100 (Fig. 2). The Interaction Network for ER-Associated Degradation (INfERAD) was arranged around clusters identified for Hrd1-SEL1L, gp78, and the mEMC subnetworks, with those components located centrally reflecting shared interactions between clusters.

As with any systems-based analysis of interaction networks, our analysis was not exhaustive, and therefore we sought to integrate data from public protein-protein interaction resources (STRING). However, as ERAD components are poorly represented in this database (Supplementary Table S5) and other online resources (BIOGRID and MINT), interactions identified in this study were instead mapped together with pair-wise interactions reported previously (Supplementary Table S5, Supplementary Fig. S5). These combined datasets contain over 250 interactions, reflecting the organisational complexity of the mammalian ERAD system.

The Hrd1-SEL1L subnetwork

Our proteomic analysis confirmed the E3 Hrd1 and its established cofactor SEL1L as a prominent nexus for ERAD. Nearly all previously reported interactions of the Hrd1-SEL1L complex (Supplementary Table S5) were validated by our dataset, which also uncovered several previously uncharacterised proteins including FAM8A1, LONP2, a putative Lon-protease (with OS-9); CPVL, a putative carboxypeptidase (with XTP3-B), the stress-inducible hemeoxygenase HMOX1/HO1 and two components of the sterol biosynthetic pathway, HMG-CoA reductase (HMGCR) and squalene synthetase (FDFT1). The rate-limiting enzyme in cholesterol synthesis, HMGCR, is subject to strict feedback regulation whereby sterol end products induce its degradation by ERAD[12,34,35]. Although evidence supports a role for gp78 in the degradation of HMGCR in mammalian cells[36], the Hrd1 pathway degrades HMGCR in both yeast (Hmg2p)[12] and *Drosophila*[37]. Identification of HMGCR as a Hrd1 HCIP lends strength to the possibility that Hrd1 also plays a role in HMGCR degradation in mammals[38].

The integrity of the Hrd1-SEL1L subnetwork was strongly influenced by solubilisation conditions. All Hrd1 HCIPs apart from FAM8A1 (Fig. 1a, cluster 1Ta) were lost in TX-100, while the complexes containing SEL1L, OS-9, and other luminal components were preserved (Fig. 1a, cluster 1Tb), consistent with all upstream (luminal) interactions being mediated via SEL1L, which is linked to Hrd1 by a TX-100-labile association[39].

The gp78 subnetwork

Cluster analysis exposed a reciprocally co-precipitating complex consisting of the E3 gp78, an uncharacterised UBA domain-containing polytopic protein UBAC2, the membrane-embedded, VCP/p97-binding protein UBXD8, and Derlins-1 and -2. The high degree of interconnectivity suggests that gp78 together with its cognate E2 (UBE2G2) and UBAC2, comprise a transmembrane pathway for ERAD that shares essential cytoplasmic (*e.g.* VCP/p97 and 26S proteasomes) and integral membrane components (UBXD8 and Derlin-2) with the Hrd1-SEL1L cluster. The recently described protein TMUB1[40] was found in the gp78 cluster, as was BRI3BP, hitherto unlinked to ER. Signal peptide peptidase (HM13/SPP) and a number of poorly characterised integral membrane proteins (TMEM201, TMEM43, LRRC59 and CLPTM1) were also linked via UBAC2. In contrast to the Hrd1-SEL1L cluster, most HCIPs associated with the gp78 subnetwork were stable in both detergents (Supplementary Table S2, S3, and S6). Disruption of the Hrd1-SEL1L cluster in TX-100 caused the shared cytoplasmic interactors VCP/p97 and UBE2G2 to cluster with gp78, likely reflecting their direct binding to the C-terminal cytoplasmic domain of gp78[41,42]. These data establish gp78 as the core of a detergent-stable E3 subnetwork that shares several components with the Hrd1 complex, and identify UBAC2 as a central element in the gp78 complex.

ERAD E3s are associated with the 26S proteasome

Strikingly, nearly all subunits of the 26S proteasome were captured with Hrd1 and gp78 in DIG lysates. Although not all of these interactions reached our stringent criteria to qualify as HCIPs (19/32 for gp78; 15/31 for Hrd1; Supplementary Table S6), the fact that gp78 captured all subunits of the 20S core particle and most subunits of the 19S regulatoryparticle

indicates a significant connection between the ERAD E3s and 26S proteasomes (Supplementary Table S6, and Fig. S6). Persistence of these interactions in TX-100 together with the observation that proteasome subunits were not identified as HCIPs of other ERAD interaction network components, suggests an intimate, perhaps direct interaction of gp78 (and possibly Hrd1) with the 26S proteasome. The excess of 20S core particle over 19S regulatory subunits captured with gp78 and Hrd1 (Fig S6) raises the possibility that E3-proteasome connections may be linked independently of the 19S regulatory particle, perhaps via direct interactions with 20S or via alternative adaptors.

The gp78 HCIP PSME4/PA200 was identified in a screen for 26S proteasome activators and originally reported as a nuclear protein with a possible role in DNA repair [45]. PA200 can assemble with 20S and 19S subunits to form hybrid 26S proteasomes[46] and a crystal structure of the apparent yeast ortholog Blm10 suggests that it interacts directly with proteasome α-subunits[47]. The functional significance of the PA200 interaction is unclear, yet its presence in gp78 (but not Hrd1) complexes suggests there may be heterogeneous 26S proteasome populations associated with the ER membrane and ERAD.

The mammalian EMC subnetwork

The detergent-stable mEMC (Fig. 1, cluster 2) was initially identified through KIAA0090, an uncharacterised, putative type I integral membrane glycoprotein detected as a Derlin-1/2 HCIP (Fig. 1 and Supplementary Table S2). With KIAA0090 as bait, we identified 5 additional HCIPs (TTC35, TMEM32/MMGT1, TMEM85, C15orf24 and COX4NB), which reciprocally co-precipitated each other, and 4 additional proteins (TMEM111, C19orf63, C14orf122, and TMEM93; Supplementary Fig. S4). The mEMC is comprised of 10 unique subunits, while its yeast counterpart appears to contain 6 (Fig. 2). Although the function of the mEMC is unknown, 3 subunits (KIAA0090, TMEM111 and TTC35) were identified as HCIPs of UBAC2 and Derlin-2, suggesting a close link between this complex and ERAD components implicated in Ub recognition and protein dislocation.

Deconvolving the ERAD interaction network with RNA interference

To begin to decipher the organisation within the mammalian ERAD interaction network, we systematically analysed the Hrd1-SEL1L and gp78 subnetworks. Coexpression of S-tagged proteins with shRNAs targeting central subnetwork nodes was used to ascertain the requirement of each component to maintain individual interactions (Fig. 3). Following SEL1L knockdown, XTP3-B interactions with Hrd1 (Fig. 3a), UBE2J1 (Fig. 3b), and FAM8A1 (Fig. 3c) were abolished, while OS-9 lost its connection to Hrd1 (Fig. 3d). LC-MS/MS analyses confirmed that XTP3-B and OS-9 affinity-purified complexes from cells lacking SEL1L lost their interactions with all downstream membrane and cytosolic components (*e.g.* Hrd1, data not shown). These data verify the essential role that SEL1L plays in scaffolding luminal, substrate-recognition elements to the Hrd1 transmembrane complex[30,39,48,49], and reveal the independent interactions of XTP3-B and OS-9 with the Hrd1-SEL1L node (Fig. 3e).

Hrd1-SEL1L subnetwork connections to integral membrane and cytosolic ERAD components differed in that SEL1L knockdown did not affect the Hrd1-FAM8A1 (Fig. 3f)

or Hrd1-UBE2J1 interactions (Fig. 3g). Similarly, loss of Hrd1 failed to sever the connections between SEL1L-UBE2J1 (Fig. 3h), SEL1L-AUP1 (Fig. 3i), or AUP1-UBE2G2 (Fig. 3j). Thus, both Hrd1 and SEL1L bind to UBE2J1, either directly or through a factor not identified in our proteomic analysis. Hrd1 knockdown abolished the SEL1L-FAM8A1 interaction (Fig. 3f), indicating that SEL1L and FAM8A1 independently bind to Hrd1. This conclusion is reinforced by the maintenance of the Hrd1-FAM8A1 interaction in TX-100 where SEL1L is lost (Fig 1). These data refine the molecular topology of the Hrd1-SEL1L complex, and identify FAM8A1, as an obligate, SEL1L-independent partner of Hrd1 (Fig. 3k).

A second prominent, highly interconnected subnetwork is composed of gp78, Derlin-2, UBAC2, and UBXD8 (Fig. 2). Knockdown of UBXD8 did not disrupt the gp78-UBAC2 interaction (Fig. 3l), nor did knockdown of gp78 affect UBXD8-UBAC2 (Fig. 3m and n). And while gp78 binding was lost, maintenance of the UBXD8-UBAC2 interaction in TX-100 indicates that their organisation occurs independently of gp78 (Fig. 1). However, the UBXD8-gp78 interaction was abrogated by knockdown of UBAC2 (Fig. 3o) but not Derlin-2 (Fig. 3p). These data allow refinement of the gp78 subnetwork topology (Fig. 3q) and identify a role for UBAC2 in the recruitment of UBXD8 to the gp78 complex.

Functional genomic analysis of ERAD components

To assess their functional roles in substrate degradation, we monitored the effect of RNAi-mediated knockdown of individual ERAD components on steady-state fluorescence levels of fluorescent ERAD substrate reporters[21,50–53]. Cell lines stably expressing GFP fusions representing three major topological classes of ERAD substrates: luminal-glycosylated (null Hong Kong variant of α1-antitrypsin (NHK)), luminal-non-glycosylated (NHK-QQQ and mutant transthyretin TTR(D18G)), and integral membrane-glycosylated (CFTRΔF508) (Fig. 4a) were employed. We also included the AMPA-type glutamate receptor subunit GluR1 as it is retained in the ER and degraded in a UPS-dependent manner (Supplementary Fig. S7). Cell lines expressing the cytosolic proteasome substrate GFP^{u}[54] and GFP served as controls for ERAD-independent effects that might alter UPS function, reporter gene expression, or GFP fluorescence.

All substrate reporter lines responded to proteasome inhibition with time-dependent increases in mean GFP fluorescence (Fig. 4b). Expression of a dominant negative VCP/p97 mutant (H317A)[52] severely impaired degradation of only the ERAD substrates, but not GFP^{u} (Fig. 4c), in agreement with the strong dependence of ERAD pathways on VCP/p97 and 26S proteasomes. The mannosidase inhibitor kifunensine (KIF) selectively inhibited the degradation of NHK (Fig. 4c), consistent with an established requirement for mannose trimming of this glycoprotein for ERAD[55,56]. GluR1 and CFTR F508 are also glycoproteins (Supplementary Fig. S7c), but were unaffected by KIF (Fig. 4c), indicating that mannose trimming is unlikely to be the dominant signal committing them to degradation, or to the existence of redundant, glycan-independent targeting for these polytopic proteins. These data reflect an implicit requirement for multiple, substrate-specific recognition elements within the ERAD interaction network to deliver substrates to shared degradation machinery.

To identify the individual factors required for substrate degradation, we generated an shRNA library targeting genes implicated in ERAD (Fig. 4d; Supplementary Table S5) and monitored their impact on the mean GFP fluorescence of reporter cell lines (Fig. 4e; Supplementary Table S7). Any shRNA that significantly stabilised an ERAD reporter was selected for further validation by rescreening through all other reporter lines and confirmation of knockdown (See Methods and Supplementary Fig. S8). Each substrate appeared to rely on a unique set of individual ERAD components for degradation (Supplementary Table S7), which is illustrated as a hierarchically clustered heat map for comparison (Fig. 4f). Of the 59 components our library targeted, only the non-ATPase subunit of the 19S regulatory particle PSMD2 and VCP/p97 were essential for all ERAD substrates (Fig. 4f). GFP^{u} was stabilised by knockdown of PSMD2, but not VCP/p97, mimicking the effects of MG132 and VCP/p97(H317A) (Fig. 4b and c) and validating the strategy of using shRNA-mediated gene silencing with ERAD reporters to interrogate the contribution of individual components to the overall degradation process. Hierarchical cluster analysis demonstrated that substrates were segregated by topology (luminal vs. integral membrane), but not by glycosylation (Fig. 4f). Moreover, a surprising degree of heterogeneity within each substrate's requirement profile was observed, especially for substrates utilising the same central ERAD components (*e.g.* Hrd1, discussed below). These characteristic patterns suggest that the ERAD system operates largely as an adaptive network, in which unique combinations of common components process individual substrates. Such an adaptive mechanism could be explained by the formation of substrate-specific subcomplexes or by a multisubunit complex that utilises discrete sets of components to achieve substrate-specific degradation.

An adaptive mechanism for Hrd1-dependent degradation

We merged the heat map of shRNA-mediated impairment for each substrate (Fig. 4f) with the comprehensive ERAD interaction network (Supplementary Fig. S5) in order to generate integrated substrate-specific snapshots of the physical and functional networks responsible for degradation (Supplementary Fig. S9–11). Loss of either E3 in the network impacted degradation in a substrate-specific manner. Hrd1 knockdown stabilised topologically disparate substrates including NHK, NHK-QQQ, TTR(D18G) and GluR1, but had little effect on GFPu or CFTRΔF508 (Fig. 4f and g). Instead, CFTRΔF508 was stabilised following gp78 knockdown, as previously reported[57]. Substrates utilising Hrd1 did not share a common dependence on Hrd1-SEL1L subnetwork components. While FAM8A1 and SEL1L were essential for degradation of NHK and TTR(D18G) and dispensable for GluR1, the converse was true for AUP1 and UBE2G2 (Fig. 4f and g). And despite sharing a common requirement for VCP/p97, ERAD substrates were differentially dependent on VCP/p97-interacting proteins such as SVIP, UBE4A and VCIP135 (Fig. 4f), perhaps indicating additional heterogeneity among the VCP/p97-containing complexes employed for dislocation.

Coordinate regulation of ERAD genes by the unfolded protein response

Expression of more than half of the ERAD genes in our network, including the Hrd1-SEL1L subnetwork (Fig. 5) and other known UPR targets (*e.g.* BiP and HERP), were induced by tunicamycin (Fig. 5). By contrast, gp78 and other ER-resident E3s responded only weakly

(Fig. 5). All but one of the mEMC components were transcriptionally upregulated by tunicamycin (Fig. 5); in yeast, only EMC3 is upregulated by the UPR[25,58]. The selective response to ER stress indicates a previously unrecognised, coordinate transcriptional regulation of this physically and functionally integrated network and suggests that the Hrd1-SEL1L and mEMC subnetworks contribute to the cellular response to ER stress and underscore an important role of ERAD in this process.

ERAD components identified within the Hrd1-SEL1L and gp78 subnetworks

FAM8A1 was identified as a previously uncharacterised component of the Hrd1-SEL1L subnetwork (Fig. 6a). Immunoprecipitation of endogenous FAM8A1 captured Hrd1 and SEL1L (Fig. 6b), confirming that FAM8A1 is a *bona fide* interactor of both components. Resistance to extraction from purified microsomes by high salt or pH support predictions for FAM8A1 as an integral membrane protein with 3 membrane-spanning domains (TOPCONS, Fig. 6c and d), while limited proteolysis of FAM8A1-containing microsomes (data not shown) and immunodetection of an N-terminal epitope tag in semipermeablised cells (Fig. 6e) established the cytoplasmic localisation of the N-terminus. A complex isolated with Stagged Hrd1 contained both FAM8A1 and SEL1L, confirming FAM8A1 as a component of this E3 ligase complex (Fig. 6f).

Disrupting the stoichiometry of the Hrd1 E3 complex by FAM8A1 knockdown (Fig. 3f) or wildtype Hrd1 overexpression (Fig. 6g) impaired degradation of TTR(D18G) while enhancing that of GluR1. TTR(D18G) degradation was restored or enhanced when Hrd1 was coexpressed with SEL1L (Fig. 6g). Similarly, FAM8A1 overexpression (or its RDD domain, a.a. 230–413) impaired TTR(D18G) but not GluR1 degradation, while a cytoplasmic N-terminal fragment (FAM8A1(Δ230–413)) affected neither (Fig. 6g). The dominant-negative effect of FAM8A1(Δ1–229) on TTR(D18G) stability implies that Hrd1 interacts with FAM8A1 via its RDD domain and that its cytoplasmic N-terminal region is required for Hrd1-mediated degradation of luminal substrates. Collectively, our results establish FAM8A1 as a binding partner and potential regulator of Hrd1-dependent ERAD.

UBAC2, identified as a UBXD8 interaction partner (Fig. 7a), is predicted to be a rhomboid family pseudoprotease similar to the Derlins[59] that also contains a putative C-terminal UBA domain. A native interaction between the two was validated by endogenous coprecipitation (Fig. 7b). Functionally, UBAC2 knockdown stabilised the Hrd1 substrate TTR(D18G)-GFP (Fig. 7c), suggesting potential coordination between the two Ub ligase complexes. Both the UBAC2 C-terminus (a.a. 304–344) and the N-terminus of UBXD8 (2–52) display a high degree of conservation with residues essential for Ub binding in UBA domains (Fig. 7d), and their predicted cytosolic localisation position them appropriately for Ub binding (Fig. 7e). While a recombinant UBAC2 C-terminal fragment (a.a. 293–344) was sufficient to capture polyUb chains from HEK293 cell lysates at a level comparable to the well-characterised hPlic2 UBA[60], under these conditions the UBXD8 UBA domain was not (Fig. 7f). Thus, it is UBAC2 rather than UBXD8 that adds polyUb-binding capabilities to the gp78 subnetwork.

DISCUSSION

The application of high-content proteomics to identify interconnectivity within defined functional networks has been used with success to map high-resolution interaction landscapes for several complex mammalian protein networks[21,22,61]. In this study, we have integrated the mammalian ERAD interaction landscape with gene expression data and substrate-specific functional “fingerprints” of the mapped components to generate a multidimensional view of this dynamic and complex network. Our data suggest that the mammalian ERAD system accommodates the diverse array of potential substrates by using combinatorial interactions of the two central E3s, Hrd1 and gp78, with a palette of accessory factors (Fig. 8).

Although many individual components of the mammalian ERAD system have been previously identified, to date there has been no systematic effort to place them into an integrated interaction landscape. Our study confirmed many of the interactions previously reported in mammals[62] and those inferred from yeast[16,63] (shown in Fig. 8; black lines), validating our approach and allowing us to arrange components into a topologically and functionally coherent model (Fig. 8). This analysis also identified 71 HCIPs that are either uncharacterised or have not previously been linked to ERAD (Fig. 8, only selected nodes and interactions shown), illustrating the ability of focused proteomic strategies to uncover novel components. Our analysis integrates interaction and functional data from the present study into a framework consisting of 6 functional modules that execute the principal ERAD activities: substrate recognition, dislocation, extraction, ubiquitination, and degradation (proteasome), as well as the EMC whose function is currently unknown. Sub-modules are grouped together based on predicted structural and topological features, and on an unbiased analysis of network interconnectivity of the proteins represented in each group. The ERAD system can thus be viewed as a distributed network, organised around central *Ubiquitin Ligase* modules for Hrd1 and gp78 that cooperate with components of the membrane-embedded *Dislocation* and the cytoplasmically-oriented *Substrate Extraction* modules. These interconnections are likely to ensure secure coupling between substrate dislocation/extraction and Ub conjugation. The Hrd1 and gp78 complexes contain sub-module-specific factors and share interactions with ERLIN1/2 and UBE2G2. The Hrd1 sub-module has four major connections to other modules. Three are mediated through SEL1L, which connects Hrd1 to the upstream luminal *Substrate Recognition* machinery, as well as to the downstream *Dislocation* module through Derlin-2 and the *Substrate Extraction* module via UBXD8. Direct interactions between the latter two proteins and VCP/p97 provide an extended pathway from the luminal substrate-binding lectins OS-9 and XTP3-B to cytoplasmic VCP/p97. The third connection is a direct link between this E3 and the 26S proteasome.

The gp78 sub-module appears to connect to the ERAD network via UBAC2. This protein interacts with UBXD8 and Derlin-1/2, and has a functional polyUb-binding domain, suggesting it may function as a membrane nexus integrating Ub conjugation, dislocation, and extraction. A VCP/p97-binding site within the cytoplasmic domain of gp78[42] means that this complex can associate with VCP/p97 in at least two ways. VCP/p97 interacts directly with multiple components of the ERAD machinery including Derlin-1 and

Derlin-2[27,59,64], VIMP[26,27], gp78[42], UBXD2[65], and UBXD8[66,67]. With at least 6 different recruitment sites for VCP/p97 within the ERAD network, it is not surprising that disruption or silencing of this cytoplasmic AAA+ ATPase has a more universal effect on the degradation of diverse ERAD substrates compared to the loss of an individual factor (Fig. 4f). Multiple recruitment avenues at the ER membrane may reflect an acquired adaptability of VCP/p97 to accommodate and engage the diverse substrates it encounters. Moreover, VCP/p97 accessory factors (*e.g.* UBE4A, VCIP135, and SVIP), functionally essential for specific substrates (Fig. 4f), could confer an added level of specificity or may reflect a requirement for different VCP/p97 configurations at different steps of the dislocation and membrane extraction processes.

"Input" of luminal substrates into the Hrd1 sub-module occurs via the well-established interaction with SEL1L. A capacity of the Hrd1 sub-module to engage substrates independently of SEL1L is also suggested by several observations: 1) SEL1L is dispensable for GluR1 degradation (Fig. 4f); 2) Hrd1 overexpression enhanced GluR1 degradation while stabilising TTR(D18G) (Fig. 6g) and 3) co-expression of SEL1L with Hrd1 resulted in enhanced degradation of both substrates (Fig. 6g). One hypothesis is that Hrd1 recognises substrates directly through its membrane-spanning region, as suggested from studies in yeast[68]. We speculate that, given its close interaction with Hrd1, FAM8A1 may regulate the partitioning of Hrd1 between SEL1L-dependent and -independent modes of substrate recognition. This model for FAM8A1 regulation of Hrd1 partitioning is supported by the opposing effects that FAM8A1 depletion has on SEL1L-dependent (A1AT(NHK), A1AT(NHK-QQQ), TTR(D18G)) and SEL1L-independent (GluR1) substrates.

How substrates are directed to the gp78 sub-module is less clear, as no high confidence interactions between components of this E3 sub-module and components of the *Substrate Recognition* module were detected in our study or have been reported. Given the large number of common components within the *Dislocation* and *Substrate Extraction* modules that interact with both E3 submodules, it is possible that these two principal ERAD E3s cooperate to degrade substrates, consistent with some ERAD substrates being partially stabilised by knockdown of either Hrd1 or gp78. Indeed several examples of cooperative function by pairs of mammalian ERAD-associated E3s have been reported, including RMA1-CHIP and RMA1-gp78 in the ubiquitination of CFTR[57,69] and also Hrd1-gp78[70].

Our data support an organisational model for ERAD where a dynamic network of interacting functional modules facilitate the recognition, recruitment, dislocation, extraction, ubiquitination, and degradation of the diverse classes of secretory pathway proteins. This work should provide a resource for future analysis of this cellular quality control system.

Supplementary Material

Refer to Web version on PubMed Central for supplementary material.

Acknowledgments

This work was supported by grants from the NIH to R.R.K. and J.W.H. J.C.C. was supported by funding from the Ludwig Institute for Cancer Research, Ltd. J.A.O. and R.E.T were supported by NRSA fellowships from NIH.

E.J.B. was supported by a fellowship from the Damon Runyon Cancer Research Foundation (DRG 1974-08). We thank the members of the Kopito lab for helpful discussion, and M. Pearce, J. Hwang, and C. Beveridge for critical reading of the manuscript.

References

1. Ghaemmaghami S, et al. Global analysis of protein expression in yeast. Nature. 2003; 425:737–741. [PubMed: 14562106]
2. Hebert DN, Bernasconi R, Molinari M. ERAD substrates: which way out? Semin Cell Dev Biol. 2010; 21:526–532. [PubMed: 20026414]
3. Buchberger A, Bukau B, Sommer T. Protein quality control in the cytosol and the endoplasmic reticulum: brothers in arms. Mol Cell. 2010; 40:238–252. [PubMed: 20965419]
4. Vembar SS, Brodsky JL. One step at a time: endoplasmic reticulum-associated degradation. Nat Rev Mol Cell Biol. 2008; 9:944–957. [PubMed: 19002207]
5. Aridor M. Visiting the ER: the endoplasmic reticulum as a target for therapeutics in traffic related diseases. Adv Drug Deliv Rev. 2007; 59:759–781. [PubMed: 17681635]
6. Xie W, Ng DT. ERAD substrate recognition in budding yeast. Semin Cell Dev Biol. 2010; 21:533–539. [PubMed: 20178855]
7. Bagola K, Mehnert M, Jarosch E, Sommer T. Protein dislocation from the ER. Biochim Biophys Acta. 2011; 1808:925–936. [PubMed: 20599420]
8. Hoseki J, Ushioda R, Nagata K. Mechanism and components of endoplasmic reticulum-associated degradation. J Biochem. 2010; 147:19–25. [PubMed: 19923195]
9. Kostova Z, Tsai YC, Weissman AM. Ubiquitin ligases, critical mediators of endoplasmic reticulum-associated degradation. Semin Cell Dev Biol. 2007; 18:770–779. [PubMed: 17950636]
10. Carvalho P, Stanley AM, Rapoport TA. Retrotranslocation of a misfolded luminal ER protein by the ubiquitin-ligase Hrd1p. Cell. 2010; 143:579–591. [PubMed: 21074049]
11. Ploegh HL. A lipid-based model for the creation of an escape hatch from the endoplasmic reticulum. Nature. 2007; 448:435–438. [PubMed: 17653186]
12. Hampton RY, Gardner RG, Rine J. Role of 26S proteasome and HRD genes in the degradation of 3-hydroxy-3-methylglutaryl-CoA reductase, an integral endoplasmic reticulum membrane protein. Mol Biol Cell. 1996; 7:2029–2044. [PubMed: 8970163]
13. Bordallo J, Plemper RK, Finger A, Wolf DH. Der3p/Hrd1p is required for endoplasmic reticulum-associated degradation of misfolded lumenal and integral membrane proteins. Mol Biol Cell. 1998; 9(1):209–222. [PubMed: 9437001]
14. Bays NW, Gardner RG, Seelig LP, Joazeiro CA, Hampton RY. Hrd1p/Der3p is a membrane-anchored ubiquitin ligase required for ER-associated degradation. Nat Cell Biol. 2001; 3(1):24–29. [PubMed: 11146622]
15. Swanson R, Locher M, Hochstrasser M. A conserved ubiquitin ligase of the nuclear envelope/endoplasmic reticulum that functions in both ER-associated and Matalpha2 repressor degradation. Genes Dev. 2001; 15:2660–2674. [PubMed: 11641273]
16. Carvalho P, Goder V, Rapoport TA. Distinct ubiquitin-ligase complexes define convergent pathways for the degradation of ER proteins. Cell. 2006; 126:361–373. [PubMed: 16873066]
17. Ravid T, Kreft SG, Hochstrasser M. Membrane and soluble substrates of the Doa10 ubiquitin ligase are degraded by distinct pathways. EMBO J. 2006; 25:533–543. [PubMed: 16437165]
18. Vashist S, Ng DT. Misfolded proteins are sorted by a sequential checkpoint mechanism of ER quality control. J Cell Biol. 2004; 165:41–52. [PubMed: 15078901]
19. Deng M, Hochstrasser M. Spatially regulated ubiquitin ligation by an ER/nuclear membrane ligase. Nature. 2006; 443:827–831. [PubMed: 17051211]
20. Mehnert M, Sommer T, Jarosch E. ERAD ubiquitin ligases: multifunctional tools for protein quality control and waste disposal in the endoplasmic reticulum. Bioessays. 2010; 32:905–913. [PubMed: 20806269]
21. Sowa ME, Bennett EJ, Gygi SP, Harper JW. Defining the human deubiquitinating enzyme interaction landscape. Cell. 2009; 138:389–403. [PubMed: 19615732]

22. Behrends C, Sowa ME, Gygi SP, Harper JW. Network organization of the human autophagy system. Nature. 2010; 466:68–76. [PubMed: 20562859]
23. Braun P, et al. An experimentally derived confidence score for binary protein-protein interactions. Nat Methods. 2009; 6:91–97. [PubMed: 19060903]
24. Riemer J, Hansen HG, Appenzeller-Herzog C, Johansson L, Ellgaard L. Identification of the PDI-family member ERp90 as an interaction partner of ERFAD. PLoS One. 2011; 6:e17037. [PubMed: 21359175]
25. Jonikas MC, et al. Comprehensive characterization of genes required for protein folding in the endoplasmic reticulum. Science. 2009; 323:1693–1697. [PubMed: 19325107]
26. Ye Y, Shibata Y, Yun C, Ron D, Rapoport TA. A membrane protein complex mediates retro-translocation from the ER lumen into the cytosol. Nature. 2004; 429:841–847. [PubMed: 15215856]
27. Lilley BN, Ploegh HL. Multiprotein complexes that link dislocation, ubiquitination, and extraction of misfolded proteins from the endoplasmic reticulum membrane. Proc Natl Acad Sci U S A. 2005; 102:14296–14301. [PubMed: 16186509]
28. Li G, Zhao G, Zhou X, Schindelin H, Lennarz WJ. The AAA ATPase p97 links peptide N-glycanase to the endoplasmic reticulum-associated E3 ligase autocrine motility factor receptor. Proc Natl Acad Sci USA. 2006; 103:8348–8353. [PubMed: 16709668]
29. Koegl M, et al. A novel ubiquitination factor, E4, is involved in multiubiquitin chain assembly. Cell. 1999; 96:635–644. [PubMed: 10089879]
30. Riemer J, et al. A luminal flavoprotein in endoplasmic reticulum-associated degradation. Proc Natl Acad Sci USA. 2009
31. Min SW, Chang WP, Sudhof TC. E-Syts, a family of membranous Ca2+-sensor proteins with multiple C2 domains. Proc Natl Acad Sci U S A. 2007; 104:3823–3828. [PubMed: 17360437]
32. Pettersson M, Bessonova M, Gu HF, Groop LC, Jonsson JI. Characterization, chromosomal localization, and expression during hematopoietic differentiation of the gene encoding Arl6ip, ADP-ribosylation-like factor-6 interacting protein (ARL6). Genomics. 2000; 68:351–354. [PubMed: 10995579]
33. Carrel D, et al. Targeting of the 5-HT1A serotonin receptor to neuronal dendrites is mediated by Yif1B. J Neurosci. 2008; 28:8063–8073. [PubMed: 18685031]
34. Goldstein JL, Brown MS. Regulation of the mevalonate pathway. Nature. 1990; 343:425–430. [PubMed: 1967820]
35. Ravid T, Doolman R, Avner R, Harats D, Roitelman J. The ubiquitin-proteasome pathway mediates the regulated degradation of mammalian 3-hydroxy-3-methylglutaryl-coenzyme A reductase. J Biol Chem. 2000; 275:35840–35847. [PubMed: 10964918]
36. Song BL, Sever N, DeBose-Boyd RA. Gp78, a membrane-anchored ubiquitin ligase, associates with Insig-1 and couples sterol-regulated ubiquitination to degradation of HMG CoA reductase. Mol Cell. 2005; 19:829–840. [PubMed: 16168377]
37. Nguyen AD, Lee SH, DeBose-Boyd RA. Insig-mediated, sterol-accelerated degradation of the membrane domain of hamster 3-hydroxy-3-methylglutaryl-coenzyme A reductase in insect cells. J Biol Chem. 2009; 284:26778–26788. [PubMed: 19638338]
38. Kikkert M, et al. Human HRD1 is an E3 ubiquitin ligase involved in degradation of proteins from the endoplasmic reticulum. J Biol Chem. 2004; 279:3525–3534. [PubMed: 14593114]
39. Christianson JC, Shaler TA, Tyler RE, Kopito RR. OS-9 and GRP94 deliver mutant alpha1-antitrypsin to the Hrd1-SEL1L ubiquitin ligase complex for ERAD. Nat Cell Biol. 2008; 10:272–282. [PubMed: 18264092]
40. Jo Y, Sguigna PV, DeBose-Boyd RA. Membrane-associated ubiquitin ligase complex containing gp78 mediates sterol-accelerated degradation of 3-hydroxy-3-methylglutaryl-coenzyme A reductase. J Biol Chem. 2011; 286:15022–15031. [PubMed: 21343306]
41. Chen B, et al. The activity of a human endoplasmic reticulum-associated degradation E3, gp78, requires its Cue domain, RING finger, and an E2-binding site. Proc Natl Acad Sci U S A. 2006; 103:341–346. [PubMed: 16407162]

42. Ballar P, Shen Y, Yang H, Fang S. The role of a novel p97/valosin-containing protein-interacting motif of gp78 in endoplasmic reticulum-associated degradation. J Biol Chem. 2006; 281:35359–35368. [PubMed: 16987818]
43. Glickman MH, Rubin DM, Fried VA, Finley D. The regulatory particle of the Saccharomyces cerevisiae proteasome. Mol Cell Biol. 1998; 18:3149–3162. [PubMed: 9584156]
44. Verma R, et al. Proteasomal proteomics: identification of nucleotide-sensitive proteasome-interacting proteins by mass spectrometric analysis of affinity-purified proteasomes. Mol Biol Cell. 2000; 11:3425–3439. [PubMed: 11029046]
45. Ustrell V, Hoffman L, Pratt G, Rechsteiner M. PA200, a nuclear proteasome activator involved in DNA repair. EMBO J. 2002; 21:3516–3525. [PubMed: 12093752]
46. Blickwedehl J, et al. Role for proteasome activator PA200 and postglutamyl proteasome activity in genomic stability. Proc Natl Acad Sci U S A. 2008; 105:16165–16170. [PubMed: 18845680]
47. Sadre-Bazzaz K, Whitby FG, Robinson H, Formosa T, Hill CP. Structure of a Blm10 complex reveals common mechanisms for proteasome binding and gate opening. Mol Cell. 2010; 37:728–735. [PubMed: 20227375]
48. Hosokawa N, et al. Human XTP3-B forms an endoplasmic reticulum quality control scaffold with the HRD1-SEL1L ubiquitin ligase complex and BiP. J Biol Chem. 2008; 283:20914–20924. [PubMed: 18502753]
49. Cormier JH, Tamura T, Sunryd JC, Hebert DN. EDEM1 recognition and delivery of misfolded proteins to the SEL1L-containing ERAD complex. Mol Cell. 2009; 34:627–633. [PubMed: 19524542]
50. Hampton RY, Koning A, Wright R, Rine J. In vivo examination of membrane protein localization and degradation with green fluorescent protein. Proc Natl Acad Sci U S A. 1996; 93:828–833. [PubMed: 8570643]
51. Fiebiger E, et al. Dissection of the dislocation pathway for type I membrane proteins with a new small molecule inhibitor, eeyarestatin. Mol Biol Cell. 2004; 15:1635–1646. [PubMed: 14767067]
52. Delabarre B, Christianson J, Kopito R, Brunger A. Central Pore Residues Mediate the p97/VCP Activity Required for ERAD. Mol Cell. 2006; 22:451–462. [PubMed: 16713576]
53. Stagg HR, et al. The TRC8 E3 ligase ubiquitinates MHC class I molecules before dislocation from the ER. J Cell Biol. 2009; 186:685–692. [PubMed: 19720873]
54. Bence NF, Sampat RM, Kopito RR. Impairment of the ubiquitin-proteasome system by protein aggregation. Science. 2001; 292:1552–1555. [PubMed: 11375494]
55. Hosokawa N, et al. Enhancement of endoplasmic reticulum (ER) degradation of misfolded Null Hong Kong alpha1-antitrypsin by human ER mannosidase I. J Biol Chem. 2003; 278:26287–26294. [PubMed: 12736254]
56. Liu Y, Choudhury P, Cabral CM, Sifers RN. Intracellular disposal of incompletely folded human alpha1-antitrypsin involves release from calnexin and post-translational trimming of asparagine-linked oligosaccharides. J Biol Chem. 1997; 272:7946–7951. [PubMed: 9065464]
57. Morito D, et al. Gp78 cooperates with RMA1 in endoplasmic reticulum-associated degradation of CFTRDeltaF508. Mol Biol Cell. 2008; 19:1328–1336. [PubMed: 18216283]
58. Travers KJ, et al. Functional and genomic analyses reveal an essential coordination between the unfolded protein response and ER-associated degradation. Cell. 2000; 101:249–258. [PubMed: 10847680]
59. Greenblatt EJ, Olzmann JA, Kopito RR. Derlin-1 is a rhomboid pseudoprotease required for the dislocation of mutant alpha-1 antitrypsin from the endoplasmic reticulum. Nat Struct Mol Biol. 2011; 18:1147–1152. [PubMed: 21909096]
60. Bennett EJ, et al. Global changes to the ubiquitin system in Huntington's disease. Nature. 2007; 448:704–708. [PubMed: 17687326]
61. Bennett EJ, Rush J, Gygi SP, Harper JW. Dynamics of Cullin-RING Ubiquitin Ligase Network Revealed by Systematic Quantitative Proteomics. Cell. 2010; 143:951–965. [PubMed: 21145461]
62. Mueller B, Klemm EJ, Spooner E, Claessen JH, Ploegh HL. SEL1L nucleates a protein complex required for dislocation of misfolded glycoproteins. Proc Natl Acad Sci U S A. 2008; 105:12325–12330. [PubMed: 18711132]

63. Goder V, Carvalho P, Rapoport TA. The ER-associated degradation component Der1p and its homolog Dfm1p are contained in complexes with distinct cofactors of the ATPase Cdc48p. FEBS Lett. 2008; 582:1575–1580. [PubMed: 18407841]

64. Oda Y, et al. Derlin-2 and Derlin-3 are regulated by the mammalian unfolded protein response and are required for ER-associated degradation. J Cell Biol. 2006; 172:383–393. [PubMed: 16449189]

65. Liang J, et al. Characterization of erasin (UBXD2): a new ER protein that promotes ER-associated protein degradation. J Cell Sci. 2006; 119:4011–4024. [PubMed: 16968747]

66. Lee JN, Zhang X, Feramisco JD, Gong Y, Ye J. Unsaturated fatty acids inhibit proteasomal degradation of Insig-1 at a postubiquitination step. J Biol Chem. 2008; 283:33772–33783. [PubMed: 18835813]

67. Alexandru G, et al. UBXD7 binds multiple ubiquitin ligases and implicates p97 in HIF1alpha turnover. Cell. 2008; 134:804–816. [PubMed: 18775313]

68. Sato BK, Schulz D, Do PH, Hampton RY. Misfolded membrane proteins are specifically recognized by the transmembrane domain of the Hrd1p ubiquitin ligase. Mol Cell. 2009; 34:212–222. [PubMed: 19394298]

69. Younger JM, et al. Sequential quality-control checkpoints triage misfolded cystic fibrosis transmembrane conductance regulator. Cell. 2006; 126:571–582. [PubMed: 16901789]

70. Bernardi KM, et al. The E3 ubiquitin ligases Hrd1 and gp78 bind to and promote cholera toxin retro-translocation. Mol Biol Cell. 2010; 21:140–151. [PubMed: 19864457]

71. Ward CL, Omura S, Kopito RR. Degradation of CFTR by the ubiquitin-proteasome pathway. Cell. 1995; 83:121–127. [PubMed: 7553863]

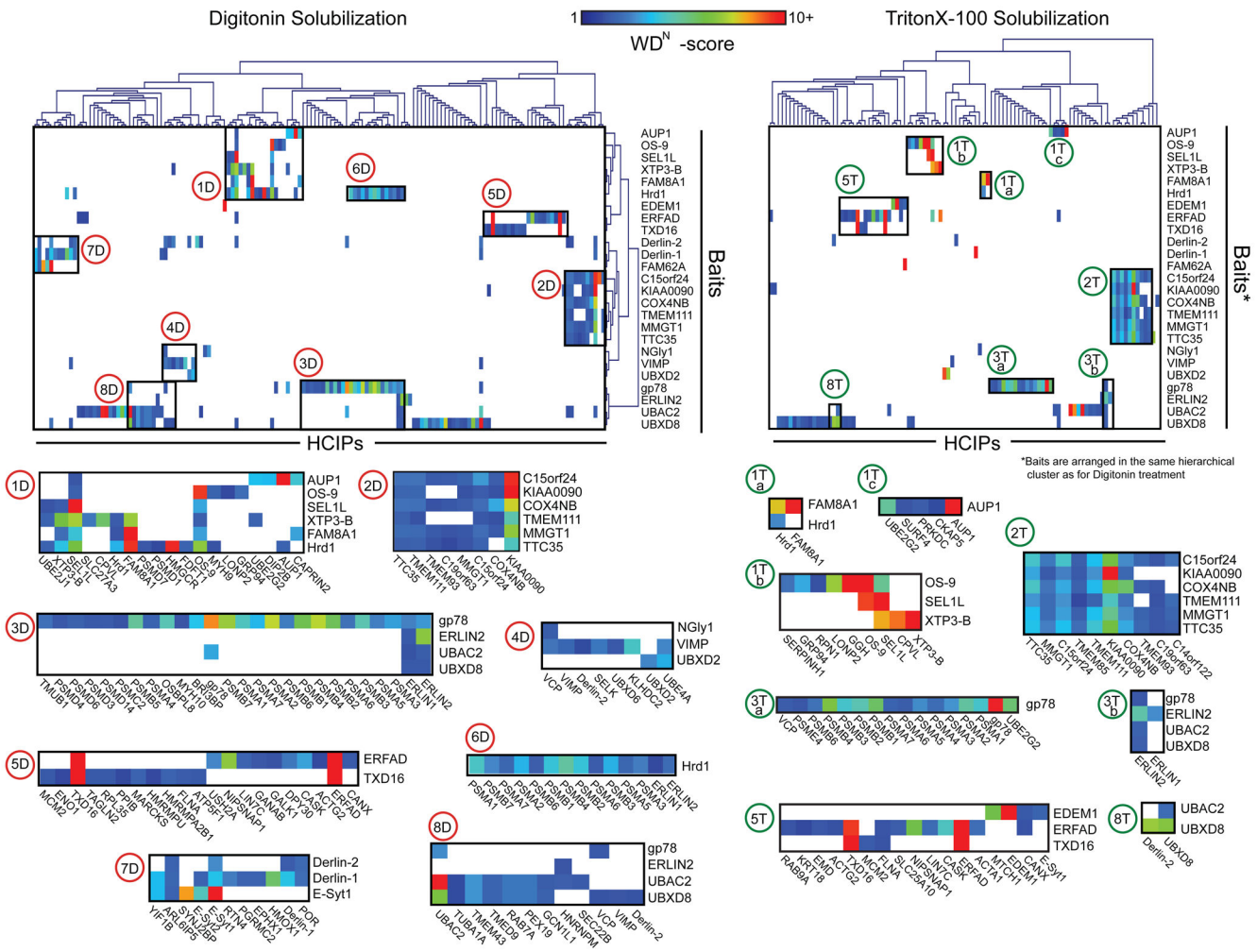

Figure 1.

Hierarchical cluster analysis of CompPASS-identified HCIPs. Hierarchical clustering of HCIPs for interactions present in DIG (left) and TX-100 (right). Prominent HCIP clusters identified in DIG (1–8D) and TX-100 (1–3, 5 and 8T) were manually selected and are highlighted below. Box colour indicates the WD^N-score.

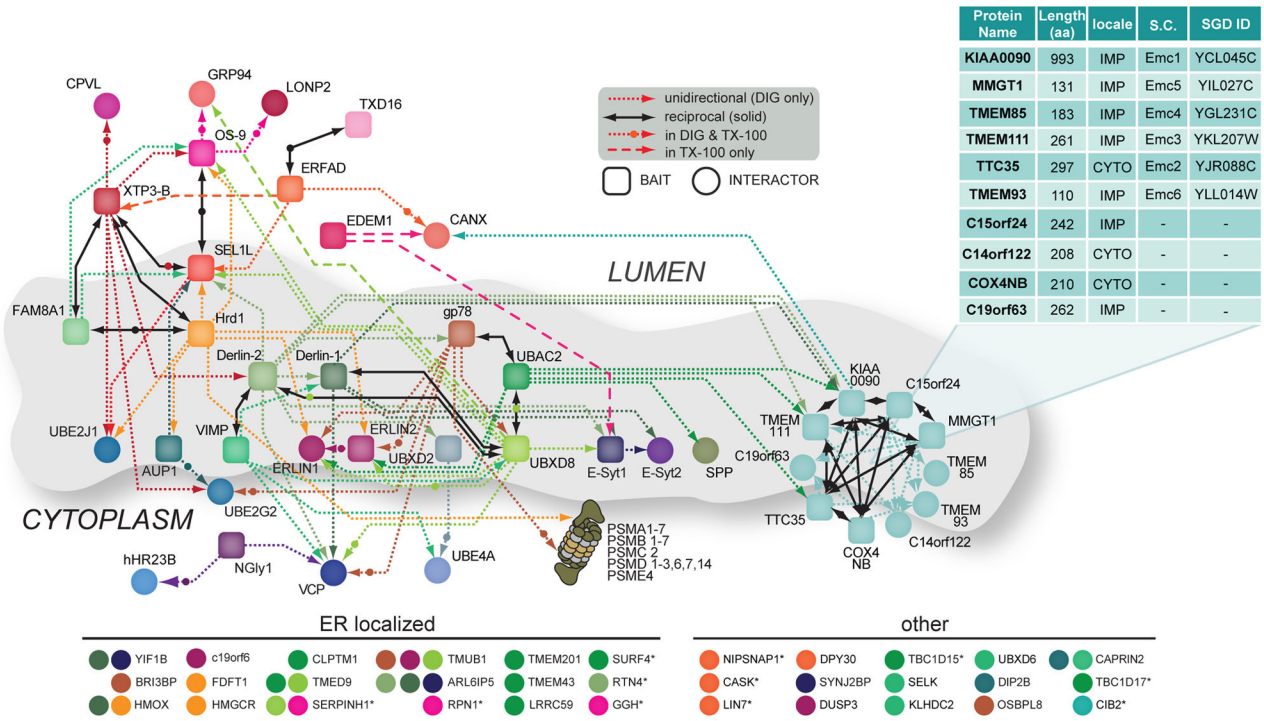

Protein Name	Length (aa)	locale	S.C.	SGD ID
KIAA0090	993	IMP	Emc1	YCL045C
MMGT1	131	IMP	Emc5	YIL027C
TMEM85	183	IMP	Emc4	YGL231C
TMEM111	261	IMP	Emc3	YKL207W
TTC35	297	CYTO	Emc2	YJR088C
TMEM93	110	IMP	Emc6	YLL014W
C15orf24	242	IMP	-	-
C14orf122	208	CYTO	-	-
COX4NB	210	CYTO	-	-
C19orf63	262	IMP	-	-

Figure 2.

The Interaction Network for ERAD (INfERAD). Interaction network for ERAD isolated in DIG and TX-100 represented by baits (squares) and their HCIPs (circles). Unidirectional (short dash, single arrow) and reciprocal (solid black, double arrows) interactions are shown. Each bait protein is rendered in a unique colour and line colour reflects the bait protein used to identify the interaction with the HCIP. Short dashed lines marked with a circle indicate interactions detected in both DIG and TX-100, while long dashed lines represent those found only in TX-100. The inset table lists the determined constituents of the mEMC, their size, cellular localisation, and corresponding yeast orthologs (SC) and ID in the Saccharomyces Genome Database (SGD). For clarity, a selection of additional DIG HCIPs not included in the map is shown on the bottom, with a circle's colour corresponding to the bait for which the HCIP was observed and asterisks denoting an HCIP also detected in TX-100.

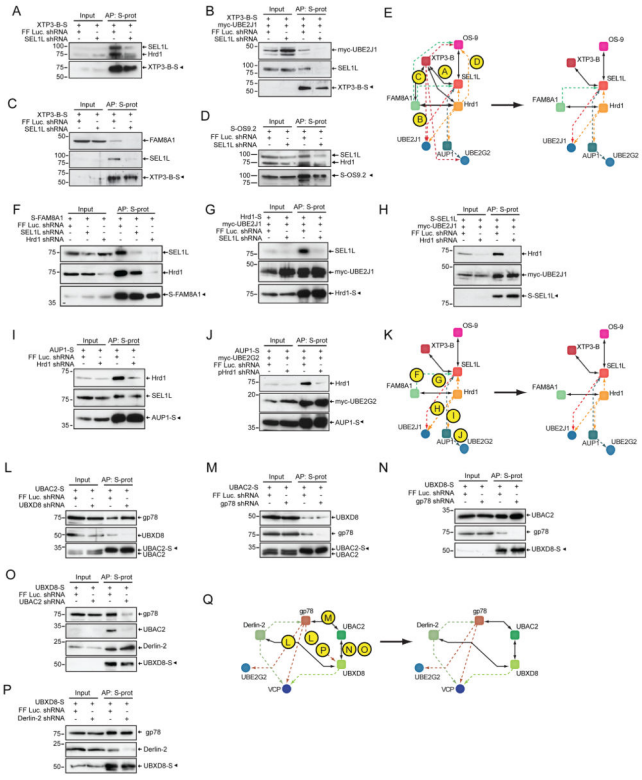

Figure 3.

shRNA-mediated refinement of Hrd1 complex interactions. (**a–q**) S-tagged ERAD baits were transiently coexpressed with the indicated shRNAs in HEK293 cells. All complexes were affinity-purified (AP) in 1% DIG and analysed by immunoblotting. (**a**) XTP3-B-S expression, probe for Hrd1 & SEL1L simultaneously; (**b**) Coexpression of myc-UBE2J1 and XTP3-B-S, probe for myc & SEL1L; (**c**) XTP3-B-S expression, probe for FAM8A1 & SEL1L; (**d**) S-OS-9 expression, probe for Hrd1 & SEL1L simultaneously; (**e**) Incorporation of refinements (**a–d**) to the Hrd1 complex; (**f**) S-FAM8A1 expression, probe for Hrd1 & SEL1L; (**g**) Coexpression of myc-UBE2J1 and Hrd1-S, probe for myc & SEL1L; (**h**) Coexpression of myc-UBE2J1 and S-SEL1L, probe for myc & Hrd1; (**i**) AUP1-S expression, probe for Hrd1 & SEL1L; (**j**) Coexpression of myc-UBE2G2, AUP1-S pulldown, probe for myc & Hrd1; (**k**) Refined interaction map for Hrd1 complex. (**l**) UBAC2-S expression with UBXD8 knockdown, probe for gp78; (**m**) UBAC2-S expression with gp78 knockdown, probe for UBXD8; (**n**) UBXD8-S expression with gp78 knockdown, probe for UBAC2; (**o**) UBXD8-S expression with UBAC2 knockdown, probe for Derlin-2, UBAC2, & gp78; (**p**) UBXD8-S expression with Derlin-2 knockdown, probe for gp78; (**q**) Refined interaction map for gp78 complex.

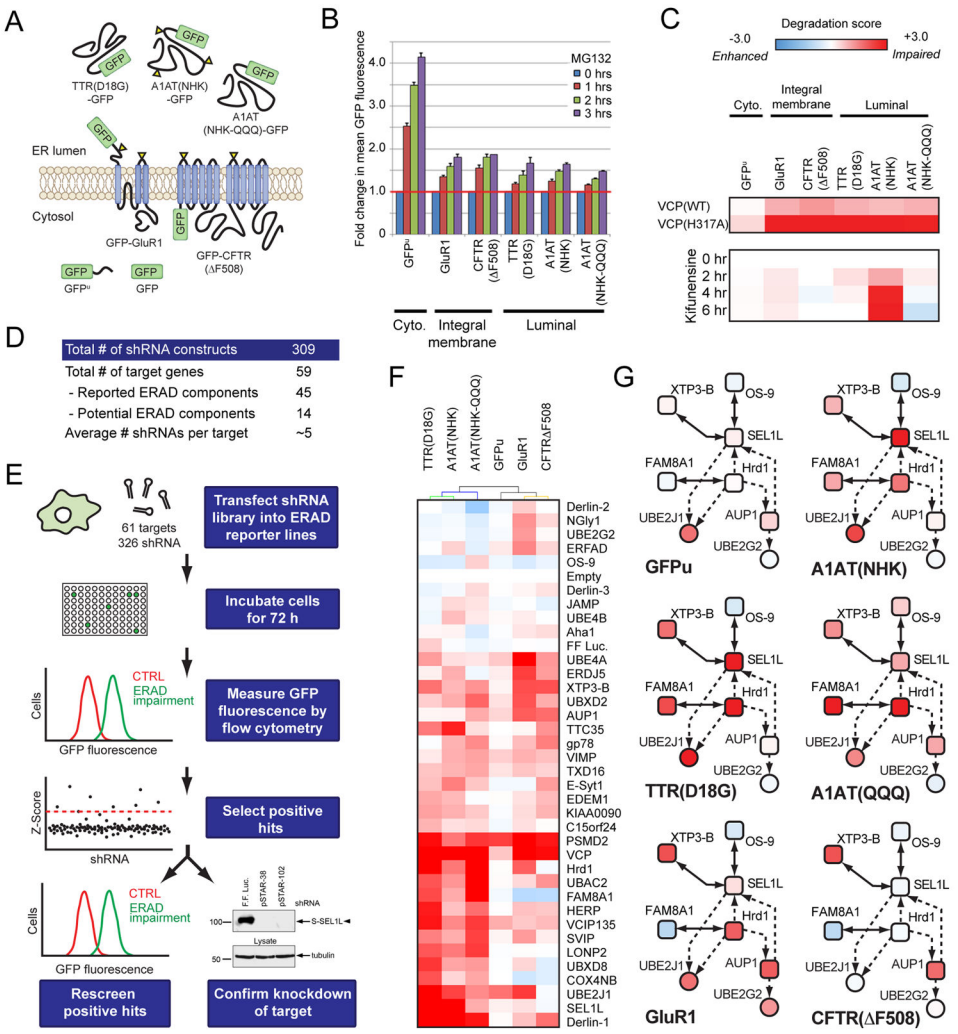

Figure 4.

Functional genomic screen to identify essential substrate-specific ERAD components. (**a**) Localisation and topology of GFP reporters; TTR(D18G)-GFP, A1AT(NHK)-GFP, A1AT(NHK_{QQQ})-GFP, GFP-GluR1, GFP-CFTR(ΔF508), and GFPu, and GFP. (**b**) Time course of relative mean GFP fluorescence levels for each ERAD reporter cell line treated with MG132 (10 μM). (**c**) Heat maps reflecting the normalised fold change in mean GFP fluorescence of ERAD reporter lines transfected with wild type or dominant-negative VCP/p97 (WT or H317A, top panel) and time course of treatment with kifunensine (30 μM, bottom panel). Fold change in mean GFP fluorescence was normalised to the levels measured for each reporter at the 3 hr time point of MG132 treatment, and thus a degradation score of 3 is equivalent to the impairment induced by 3 hr MG132 treatment. (**d**) Target composition of the shRNA library. (**e**) Overview of the functional genomic screen. (**f**) Hierarchically clustered heat map of the normalised fold change in mean GFP fluorescence of ERAD reporter lines in response to shRNA-mediated knockdown of ERAD components. The normalisation and colour scale are the same as in panel (**c**). (**g**) Functional data from the heat map shown in panel F were mapped onto the refined Hrd1 physical

interaction network (Fig. 3k) to provide an integrated snapshot of substrate-specific functional requirements for Hrd1 network components.

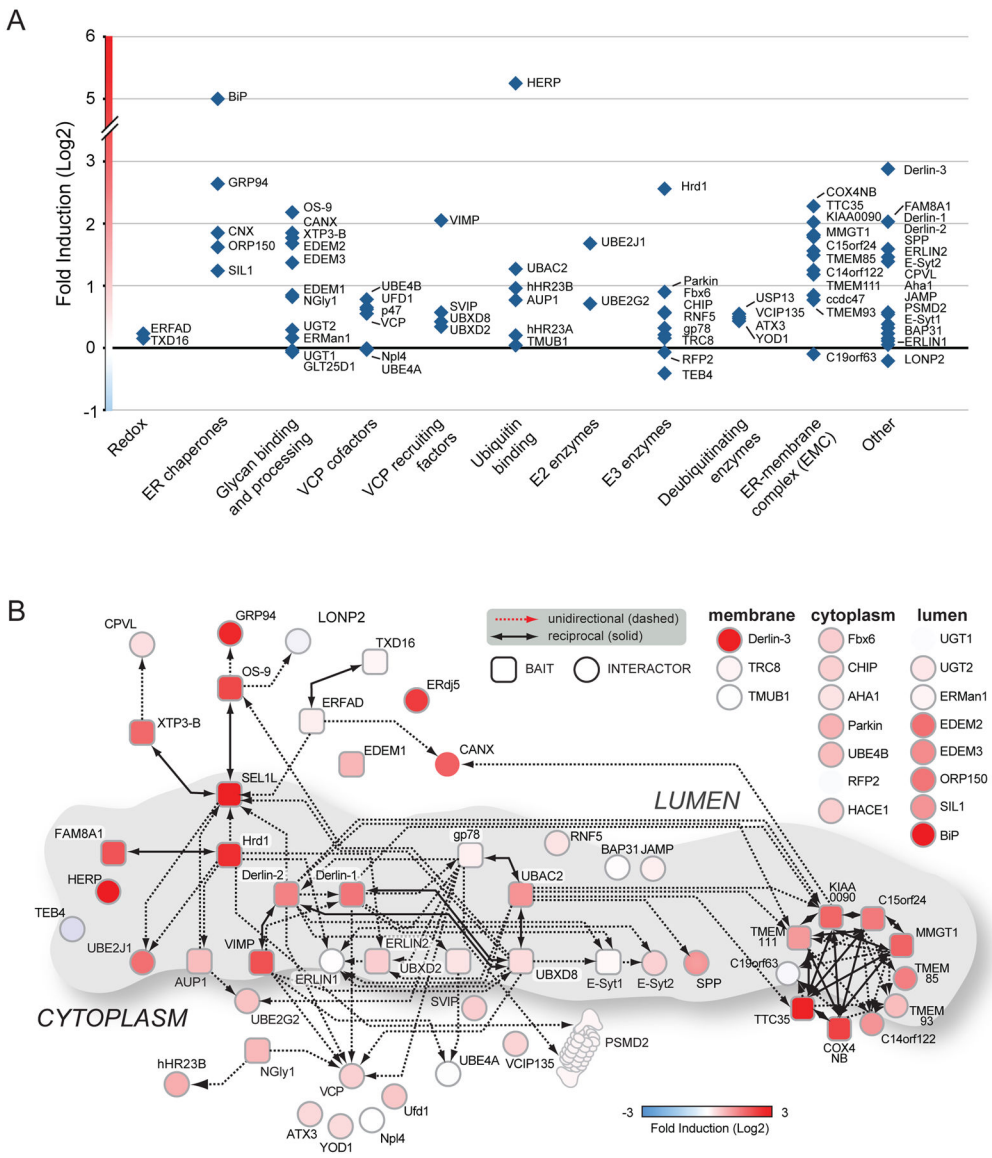

Figure 5.

Coordinated ER stress response of ERAD genes. qRT-PCR results for validated and suspected ERAD components upon treatment of HEK293 cells with TUNIC (10μg/mL, 6 hr). Data are presented as fold induction (log2) normalised to β-Actin. TUNIC-induced expression changes in ERAD genes plotted as groups according to: (**a**) Fold induction of gene expression represented by functional category. (**c**) Fold induction of gene expression from panel (**b**) mapped onto the ERAD interactome from Fig. 2b. Additional genes of interest are presented alongside the induction map.

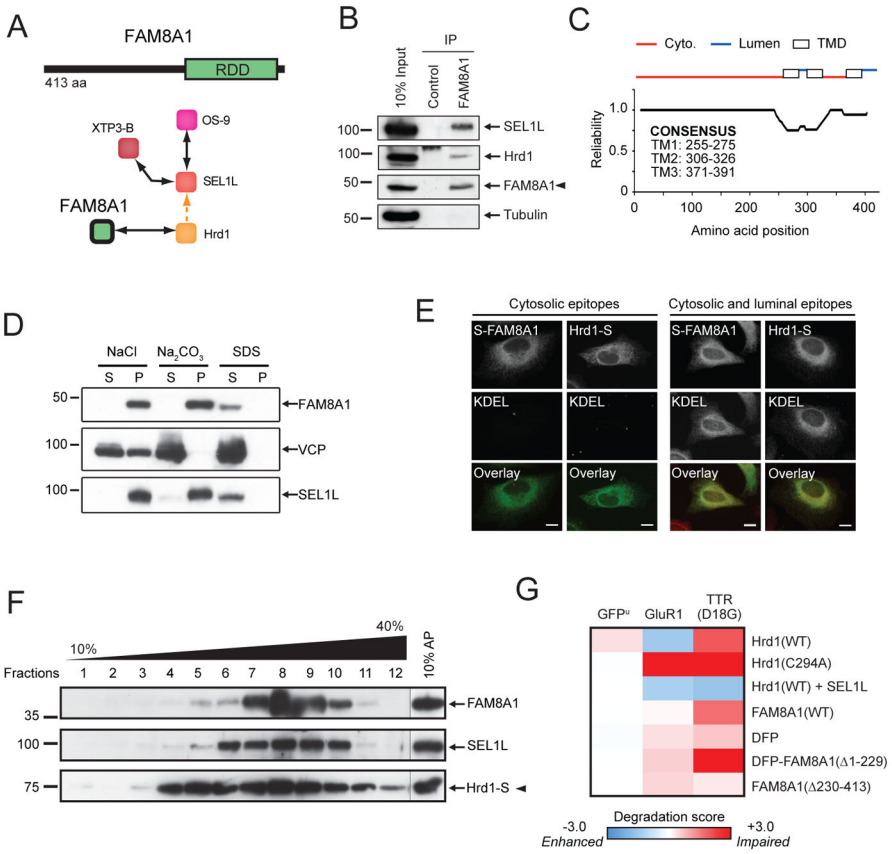

Figure 6.

Characterisation of the novel Hrd1-binding partner FAM8A1. (**a**) Domain structure and interaction network of FAM8A1. (**b**) Immunoprecipitation with anti-FAM8A1 from HEK293 DIG soluble lysates were analysed by immunoblotting with the indicated antibodies. (**c**) Consensus TOPCONS prediction of FAM8A1 membrane orientation (http://topcons.cbr.su.se). Reliability index indicates the likelihood for consensus prediction at each position using a sliding 21 amino acid window. (**d**) HEK293 membrane fractions incubated with 1 M NaCl, 0.1 M Na_2CO_3 pH 12, or 1% SDS. Following 100,000xg centrifugation, equal volumes of soluble (S) and pellet (P) were analysed by Western blot with anti-FAM8A1. (**e**) HeLa cells expressing S-FAM8A1 or Hrd1-S were permeabilised with DIG or TX-100 to allow antibody access to cytosolic epitopes or cytosolic and luminal epitopes, respectively, immunostained and analysed by fluorescence microscopy. Scale bar = 10 μm. (**f**) Hrd1-S expressing HEK293 cell lysates separated on a continuous 10–40% sucrose gradient. S-tagged Hrd1 protein complexes were affinity-purified from each 1 mL fraction (fractions 1–12) or from 150 mg whole cell lysate (10% AP), and analysed by Western blotting for Hrd1 (S-tag), SEL1L, and FAM8A1. (**g**) Heat map representing the normalised change in mean GFP fluorescence (20,000 cells, n=3) of the indicated ERAD reporter cell lines to transfection with the indicated Hrd1, SEL1L, and FAM8A1 plasmids. DFP indicates dead fluorescent protein, a non-fluorescent GFP variant. Data is represented as a normalised heat map as in Fig. 4c.

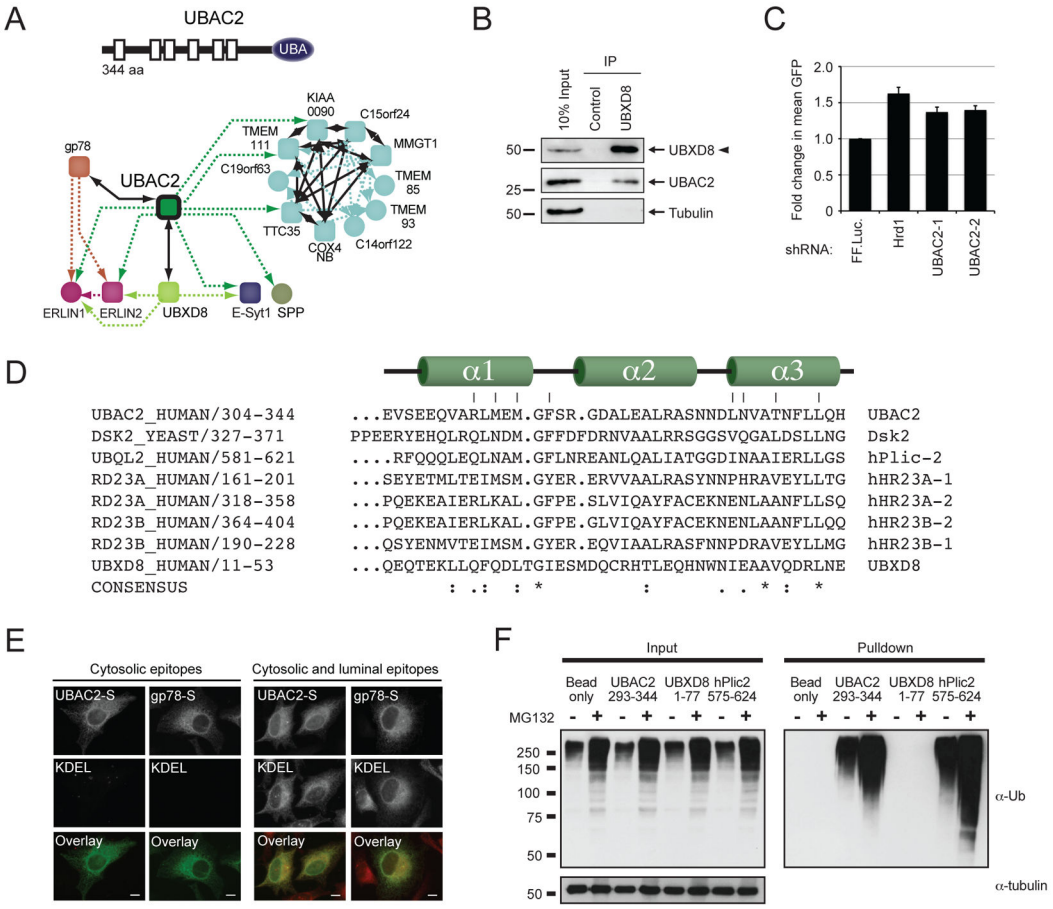

Figure 7.

Characterisation of UBAC2, a novel ubiquitin-binding ERAD component. (**a**) Predicted domain structure and interaction network of UBAC2. (**b**) Immunoprecipitation with anti-UBXD8 from HEK293 DIG soluble lysates were analysed by Western blotting with the indicated antibodies. (**c**) Analysis of muliple UBAC2 targeting shRNAs on the Hrd1 substrate TTR(D18G)-GFP by flow cytometry. (**d**) Sequence alignment of the predicted UBA domains from UBAC2 (304–344) and UBXD8 (8–53) with characterised human and yeast UBA domains. (**e**) HeLa cells expressing C-terminally S-tagged UBAC2 or gp78 were permeablised, immunostained, and analysed by fluorescence microscopy as in Figure 1e. (**f**) Recombinantly expressed UBA domains of hPlic2, UBXD8, and UBAC2 were coupled to Affigel and incubated with HEK293 cell lysates (−/+ 10 μM MG132, 6 hr). Samples were separated by SDS-PAGE, and ubiquitin binding was determined by immunoblotting with anti-Ub.

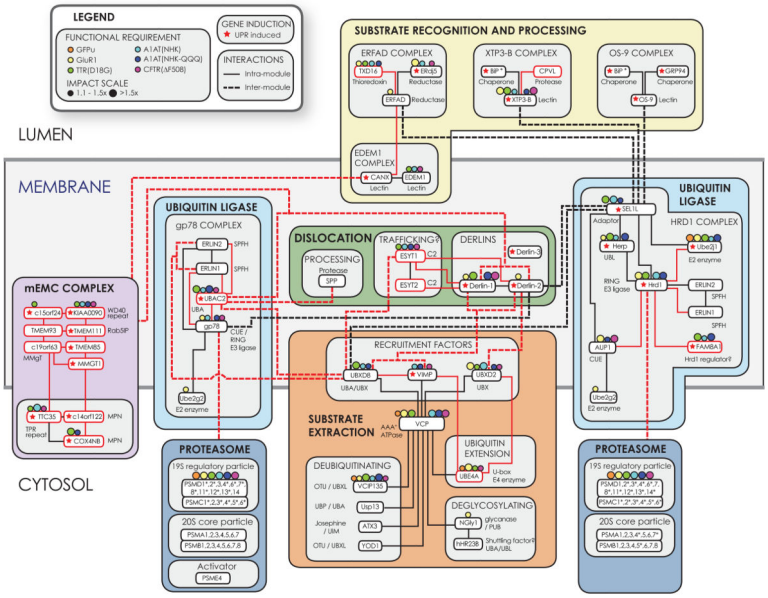

Figure 8.

Functional integration of mammalian ERAD networks. The schematic model of the ERAD protein interaction network is topologically organised with respect to the ER membrane and arranged as an array of 6 colour-coded functional modules. Individual components from this study (baits or HCIPs) are indicated as nodes with reported components (*black*) and novel components (*red*). Similarly, reported interactions confirmed in this study (*black*) and novel interactions (*red*) are shown. Symbols for protein-protein interactions, UPR induction, and functional requirements are indicated in the legend. Intermodule interactions represented terminate either at the specific node within a module that establishes the link with the module periphery or at the module itself (where there are interactions with multiple components and that module is a single complex, (*e.g.* the mEMC or proteasome)). Asterisks indicate components that were identified by proteomics, but exhibited a subthreshold CompPASS score (WD^N-score < 1.0).